

Interplay between Spin-Density Wave and Proximity Magnetic Layers

Zhu-Pei Shi and R. S. Fishman

Solid State Division, Oak Ridge National Laboratory, Oak Ridge, Tennessee 37831-6032

(Received 21 August 1996)

A spin-density wave (SDW) is shown to mediate a strongly temperature-dependent magnetic coupling between magnetic proximity layers. For parallel or antiparallel moments in the proximity layers, the order parameters of the SDW oscillate as a function of the spacer thickness with a two monolayer period. The SDW phase transition between incommensurate and commensurate phases can be controlled by flipping the magnetization of one of the proximity layers. [S0031-9007(97)02435-6]

PACS numbers: 75.70.Cn, 75.30.Ds, 75.30.Fv

Spin-density waves (SDW) have been the subject of intensive study for many years [1]. While the SDW in bulk Cr is incommensurate (I), a commensurate (C) SDW can be stabilized by doping. Recently, the SDW phase in thin films or in the spacers of magnetic multilayers has received a great deal of attention. In scanning electron microscopy with polarization analysis (SEMPA) studies [2], Cr films on Fe substrates exhibit an I SDW even well above the Néel temperature $T_N \sim 311$ K of bulk Cr. Although the SEMPA study cannot distinguish whether the observed SDW is induced by the magnetic coupling with the Fe proximity layers or by the strong Fermi-surface nesting in Cr, perturbed angular correlation spectroscopy on Fe/Cr multilayers [3] attributes the magnetic behavior of the Cr spacer to the intrinsic antiferromagnetism of bulk Cr. First-principles calculations have shown that the oscillatory magnetic coupling between two Fe layers can be explained by either paramagnetic or antiferromagnetic Cr spacers [4]. Despite these remarkable studies, the relationship between the interface coupling and bulk SDW magnetism is still poorly understood. In this Letter, we study the competition between the bulk SDW antiferromagnetism of a Cr spacer and the magnetic coupling at the interfaces. As described below, this competition affords a novel way to select the I and C SDW phases by switching the magnetic configurations of the proximity magnetic layers.

The SDW in bulk Cr is produced by the coherent motion of electrons and holes coupled by the Coulomb interaction [5]. Although usually believed to coincide with the Fermi surface nesting wave vectors $Q_{\pm} = (2\pi/a)(1 \pm \delta)$, the SDW ordering wave vectors are

actually given by [6] $Q'_{\pm} = Q_{\pm} \mp \Lambda \delta 2\pi/a$, where a is the lattice constant of the conventional bcc unit cell. For pure Cr, $\delta \approx 0.05$ [7] so that the hole Fermi surface is somewhat larger than the electron Fermi surface. When $\Lambda = 0$, the SDW wave vector equals the nesting wave vector; when $\Lambda = 1$ the SDW is commensurate with the underlying lattice. In order to minimize the nesting free energy ΔF , $0 < \Lambda \leq 1$ so the SDW wave vectors Q'_{\pm} lie closer to $2\pi/a$ than the nesting wave vectors Q_{\pm} . If the SDW wave vector lies along the \hat{z} direction normal to the multilayer interface, the spin at each atomic layer can be written

$$\mathbf{S}(z) = \hat{m} \alpha_s g (-1)^{2z/a} \cos\left[\frac{2\pi}{a}(1 - \Lambda)\delta z - \theta\right], \quad (1)$$

where α_s is a constant, θ is an arbitrary phase, g is an order parameter, and $\alpha_s g = 0.6\mu_B$ for bulk Cr at zero temperature.

For a spacer consisting of N ML's sandwiched by two ferromagnetic layers with moments \mathbf{S}_M , the coupling between the spacer and the magnetic layers may be approximated by an interaction of the form of $\mathbf{S}_M \cdot \mathbf{S}(z)$ at interfaces I ($z = 1$) and II ($z = N$). Assuming that the order parameters of the SDW are the same for each atomic layer in the spacer, the energy of the SDW per interface area a^2 is given by E/a^2 with

$$E = A\mathbf{S}_M^I \cdot \mathbf{S}(1) + A\mathbf{S}_M^{II} \cdot \mathbf{S}(N) + \Delta F a^3 (N - 1)/2. \quad (2)$$

Here $A > 0$ is the antiferromagnetic coupling constant at the interface and z is measured in units of $a/2$. The free energy per unit volume ΔF of the spacer at temperature T can be constructed with a Green's function approach [6]:

$$\Delta F(\varepsilon_0, g, \Lambda, T) = \rho_{eh} g^2 \ln\left(\frac{T}{T_N^*}\right) + \rho_{eh} \sum_{n=0}^{\infty} g^2 \frac{1}{n + 1/2} - \rho_{eh} \sum_{n=0}^{\infty} T \int_{-\infty}^{+\infty} d\varepsilon \ln \left| 1 - g^2 \frac{2i\omega_n - \varepsilon_0 + 2\varepsilon}{(i\omega_n - \varepsilon)[(i\omega_n - \varepsilon_0/2 + \varepsilon)^2 - (\varepsilon_0(\Lambda - 1)/2)^2]} \right|, \quad (3)$$

where $\omega_n = (2n + 1)\pi T$ are the Matsubara frequencies, ρ_{eh} is the electron-hole density of states, and $T_N^* \approx 80$ meV is the Néel temperature for a perfectly nested Cr alloy with $\delta = 0$. The energy mismatch $\varepsilon_0 = 4\pi\delta v_F/\sqrt{3}a$ between

the electron and hole Fermi surfaces ($v_F \approx 2600$ meV Å is the Fermi velocity) will decrease with Mn doping and increase with V doping. This expression for the free energy of the spacer should be valid for $N \geq 10$ ML's.

After fixing the magnetic configurations of the proximity magnetic layers, the SDW order parameters g and Λ as well as the arbitrary phase θ are chosen to minimize the energy E in Eq. (2). For simplicity, we consider magnetic layers which are either ferromagnetically (F) or antiferromagnetically (AF) arranged so that the SDW is linearly polarized with \hat{m} parallel to \mathbf{S}_M [8]. Then $\mathbf{S}(1) = \mathbf{S}(N)$ and $\mathbf{S}(1) = -\mathbf{S}(N)$ for F and AF arranged magnetic layers, respectively. The corresponding energies of the multilayer are

$$E_F = -2A\alpha_s g S_M |\cos\phi| + \Delta F(g, \Lambda, T) a^3 (N-1)/2, \quad (4)$$

$E_{AF} = -2A\alpha_s g S_M |\sin\phi| + \Delta F(g, \Lambda, T) a^3 (N-1)/2$, where $\phi = (\pi/2)(N-1)[1 + (1-\Lambda)\delta]$. In numerical calculations, we use the parameters $\delta = 0.05$ and $\varepsilon_0 = 5T_N^*$ of bulk Cr. The SDW order parameter is restricted to values below the bulk maximum of $g_{\max} = 1.246T_N^*$, which is achieved in the C SDW phase of a bulk Cr alloy at $T = 0$. Upon normalizing the energy by $\rho_{\text{eh}} T_N^{*2}$, we are left with the lone dimensionless coupling constant $\gamma = A \alpha_s S_M / (\rho_{\text{eh}} T_N^{*2})$ [9].

Beyond shifting the SDW amplitude and wave vector, the interfacial interactions are expected to affect the electron-hole pairs at the interface in a complex fashion. However, corrections to the energies of Eq. (4) can be safely neglected because the coherence length of the electron-hole pairs in Cr is so short. In analogy with the result for a BCS superconductor [10], the pair coherence length is given by $\xi_0 = \hbar v_F / \pi \Delta_0 \approx 4.3 \text{ \AA}$, where $\Delta_0 \approx 190 \text{ meV}$ is the energy gap of the C SDW. So the SDW order parameters will be modified only within two or three monolayers from the Fe interface. This behavior has been confirmed by the recent first-principles calculations of Mirbt *et al.* [11]. While the change in the SDW order parameters near the interfaces will somewhat enhance the coupling constant γ , the predictions of our model are otherwise unaffected.

We first evaluate the bilinear magnetic coupling $J_{\text{coup}} = E_{AF} - E_F$ as a function of temperature T and thickness N . Taking $\gamma = 1$ and $T = 0.5T_N$, we plot J_{coup} as a function of spacer thickness in Fig. 1(a). As expected, J_{coup} oscillates between F (>0) and AF (<0) values with a short 2 ML period. Above the Néel temperature, the magnetic coupling quickly decreases with increasing spacer thickness as demonstrated in Fig. 1(b). The overall coupling patterns shown in Fig. 1 resemble those observed in Fe/Cr systems [2].

Fixing the thickness of the spacer, we also evaluate the magnetic coupling as a function of temperature. For $N = 25$ and $\gamma = 1$, J_{coup} is plotted as the dashed curve in Fig. 2. Notice that J_{coup} decreases by a factor of 2 as the temperature increases to T_N , and becomes weakly F above $1.41 T_N$. The corresponding F and AF energies of the SDW are plotted in Fig. 2 as the solid and dotted curves, respectively. As implied by the peak in E_F at $0.89 T_N$, the SDW undergoes a first-order phase transition [1] from the I phase ($\Lambda \approx 0.05$) to the C phase ($\Lambda = 1$).

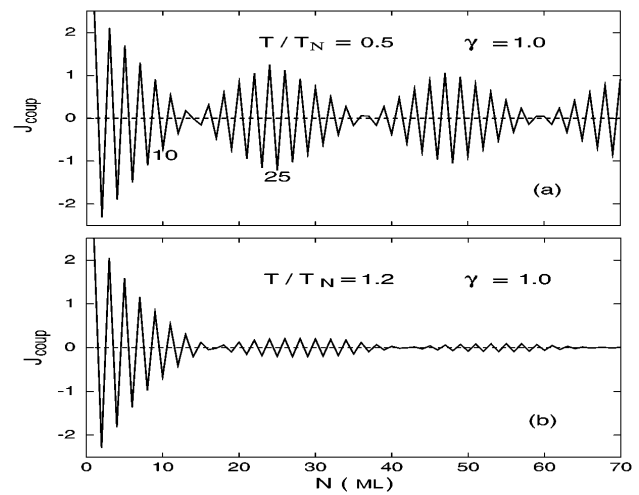


FIG. 1. Bilinear magnetic coupling as a function of spacer thickness for $\gamma = 1$ and (a) $T = 0.5T_N$ or (b) $T = 1.2T_N$.

The same features are obtained using different effective coupling constants e.g., $\gamma = 2.5$. A physical explanation for this phase transition is provided below.

Because the temperature is much less than the Fermi energy, the conventional RKKY coupling mediated by spin-polarized electronic states has very little temperature dependence. Although the temperature dependence of the RKKY coupling has been verified in magnetic multilayers with nonmagnetic spacers [12], it can *not* explain the strongly temperature-dependent magnetic coupling observed in some magnetic multilayers with Cr and Mn spacers [13,14]. At least qualitatively, our model explains the decrease in the AF coupling strength in Fe/Cr multilayers by a factor of two between 50 and 350 K [13] and the disappearance of the AF coupling above 320 K in Co/Mn multilayers [14].

Clearly, the proximity magnetic layers will modify the SDW order parameters of the spacer. In the absence

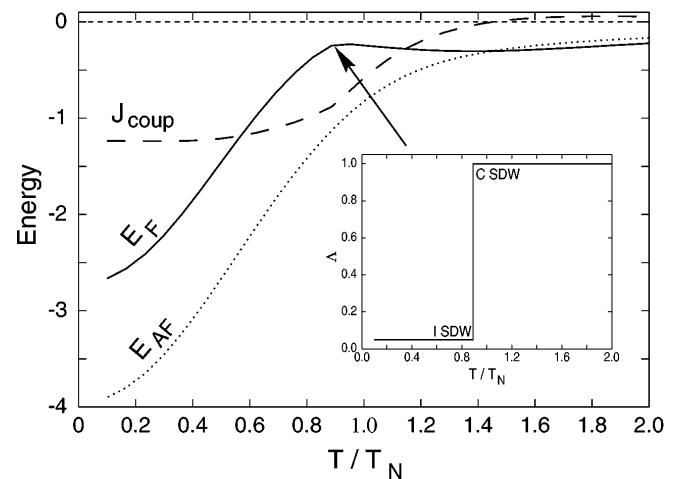


FIG. 2. Magnetic energies as functions of temperature for $\gamma = 1$ and $N = 25$ ML. Inset: The wave vector parameter Λ of the SDW as a function of temperature for F arranged magnetic layers.

of interface coupling ($\gamma = 0$), the bulk values of the SDW amplitude g and wave vector Λ are evaluated by minimizing ΔF in Eq. (3). If $T = 0.5T_N$, then $g_{\text{bulk}} = 0.647T_N^*$ and $\Lambda_{\text{bulk}} = 0.125$. When $\gamma > 0$, the SDW order parameter g always exceeds its bulk value. After fixing the magnetic configurations of the proximity magnetic layers, we find that both order parameters oscillate as a function of the spacer thickness with a 2 ML period and approach their bulk values as $N \rightarrow \infty$. For F arranged magnetic layers with $T = 0.5T_N$ and $\gamma = 2.5$, g and Λ are given by the dotted lines of Figs. 3 and 4, respectively. While g and Λ jump between lower and higher values with a period of 2 ML, their oscillation patterns shift at spacer thicknesses of 34, 51, and 74 ML.

The striking features in Figs. 2–4 can be explained by the competition between the interface coupling, which maximizes the SDW amplitude at the boundaries, and the intrinsic antiferromagnetism of the spacer, which favors the bulk values of the SDW amplitude and wave vector. While the SDW gains energy $2A\alpha_s S_M g |\cos\phi(N, \Lambda)|$ or $2A\alpha_s S_M g |\sin\phi(N, \Lambda)|$ due to the interactions at interfaces, it forfeits energy $[\Delta F(g, \Lambda) - \Delta F(g_{\text{bulk}}, \Lambda_{\text{bulk}})]a^3(N - 1)/2$ due to the changes in the order parameters of the spacer. When $\Lambda = 1$, $|\cos\phi| = 1$ and $|\sin\phi| = 0$ for odd N while $|\cos\phi| = 0$ and $|\sin\phi| = 1$ for even N . Hence the interactions at the interfaces with F (AF) moments prefer a C (I) SDW in a spacer with odd N and an I (C) SDW in a spacer with even N . If $\Delta F = 0$, the interface coupling always favors a C SDW state with $|\cos\phi|$ or $|\sin\phi|$ equal to one. So as shown in Fig. 2 for $N = 25$, the C SDW is stabilized and the F coupling is favored at a high enough temperature that the bulk free energy $\Delta F(g, \Lambda)$ is sufficiently small.

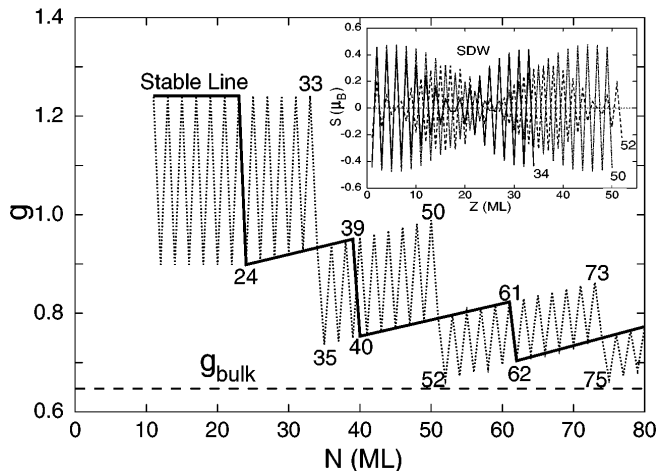


FIG. 3. SDW amplitude g in units of T_n^* as a function of spacer thickness for $T = 0.5T_N$ and $\gamma = 2.5$. The dotted line is for F arranged magnetic layers, and the solid line is for the stable magnetic configuration (F or AF) with the lowest energy. Selected thicknesses are displayed. Inset: SDW profiles in the spacer for $N = 34$ ML (solid), 50 ML (dotted), or 52 ML (dashed).

As the spacer thickness increases for odd or even N in Figs. 3 and 4, the SDW first stretches to optimize the interface coupling and then suddenly relaxes to lower the bulk free energy. For example, the SDW with $N = 34$ ML drawn as the solid curve in the inset to Fig. 3 contains a single node. As even N increases, the SDW stretches until it attains the profile of the dotted curve for $N = 50$ ML. With the addition of two more ML's, two new nodes appear in the SDW profile (dashed curve for $N = 52$ ML) and the SDW amplitude drops towards its bulk value. As N increases further, the cycle of stretching and relaxing repeats with a period close to the wavelength ~ 40 ML of the bulk SDW. For odd N , the same cycle is offset by about 20 ML. So the jumps in the SDW order parameters at 34, 51, and 74 ML are also separated by about 20 ML. The inset to Fig. 4 indicates that these thicknesses coincide with the maxima in the F energies.

For AF arranged magnetic layers, the oscillation patterns for g and Λ plotted in Figs. 3 and 4 are shifted to the right by one ML. The dotted and dashed lines in the inset of Fig. 4 then represent E_{AF} for even and odd N , respectively. As shown in the inset to Fig. 4, the SDW order parameters relax at the same thicknesses where $|J_{\text{coup}}|$ is a local maximum. The order parameters g and Λ corresponding to the lowest energy magnetic configurations (F or AF) of the proximity magnetic layers are plotted in the solid “stable line” in Figs. 3 and 4, respectively. So for N between 24 and 39, the F (AF) configuration is stable for even (odd) N while for N between 40 and 61, F (AF) configurations are stable for odd (even) N . The steps on the stable line of the order parameters at the spacer thickness of 23, 39, and 61 ML correspond to the nodes of J_{coup} as indicated by the inset of Fig. 4.

Using neutron scattering to study Fe/Cr superlattices, Fullerton *et al.* [15] recently estimated the SDW periods

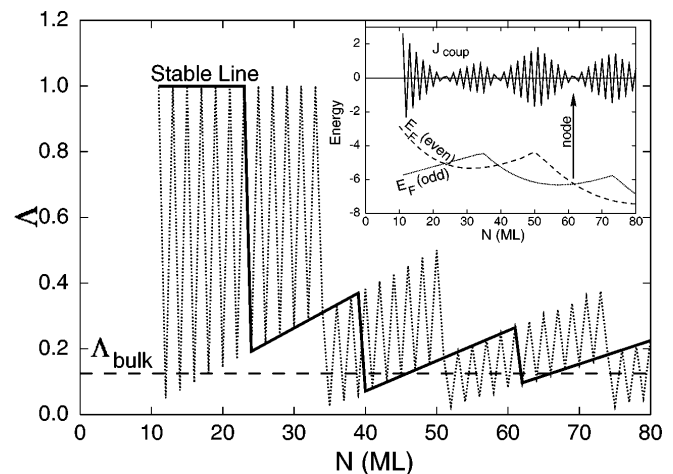


FIG. 4. Wave vector parameter Λ as a function of spacer thickness for the same parameters as in Fig. 3. Inset: Magnetic energies as a function of the spacer thickness for odd (dotted) or even (dashed) N . The bilinear coupling is also drawn as the solid line.

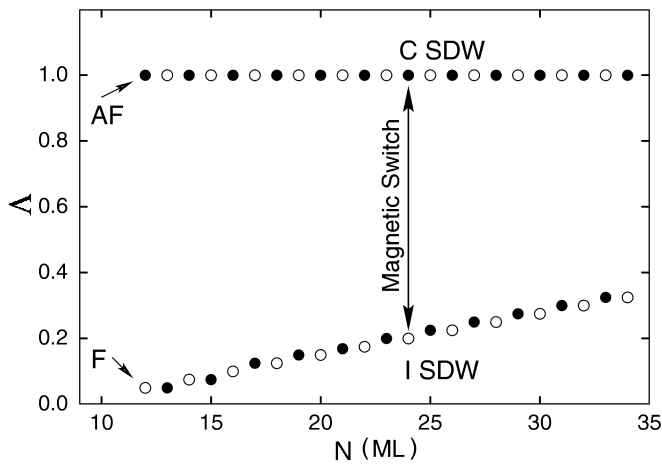


FIG. 5. Wave vector parameter Δ as a function of spacer thickness for the same parameters as in Fig. 3. Solid and empty dots are calculated data for AF and F configurations of proximity magnetic layers, respectively.

for several thicknesses of Cr spacers. Their data can be well-described by a rigid SDW as in Eq. (1). Because interfacial roughness suppresses antiferromagnetic order, the nodes of the SDW are found to lie at the interfaces and the Néel temperature is found to vanish for thicknesses less than about 30 ML. By contrast, the coupling $\mathbf{S}_M \cdot \mathbf{S}$ maximizes the magnetic order at the smooth interfaces assumed in this Letter and observed in Ref. [16]. Despite this important distinction, Ref. [15] observes a C to I SDW transition between 21 and 35 ML like the one predicted along the stable line in Fig. 4. Unfortunately, the large error bars (of about 10%) reported for the I SDW period do not permit a detailed comparison with the oscillation pattern predicted in Fig. 4.

Finally, we introduce a *magnetic switch* to select the I and C SDW phases by changing the magnetic configurations of the proximity magnetic layers. Traditionally, a transition between the I and C phases may be produced only in a narrow range of impurity concentrations by carefully tuning the temperature [1]. In Fig. 5, we show that such a phase transition can be achieved by simply flipping the magnetization of the proximity magnetic layers between F and AF configurations. Since the spin excitations of I and C SDW phases are quite different [17], this technique may provide a practical method to nano-engineer the spin dynamics of thin films.

In conclusion, we have studied the interplay between SDW magnetism and the coupling with proximity magnetic layers. Because of the change in its wave vector, the SDW produces a temperature-dependent magnetic coupling between the proximity layers. Neutron-scattering measurements should be able to confirm the predicted stretching and relaxation of the SDW order parameters as a function of spacer thickness. A novel approach to select the I and C SDW phases in the spacer by switching the magnetic configurations of the proximity layers is presented.

We would like to thank Dr. Zhenyu Zhang for a critical reading of this manuscript and Dr. John F. Cooke and Dr. Sam Liu for helpful discussions. This research was supported by Oak Ridge National Laboratory, managed by Lockheed Martin Energy Research Corp. for the U.S. Department of Energy under Contract No. DE-AC05-96OR22464, and by Oak Ridge Institute for Science and Education (ZPS).

Note Added.—Since submitting this paper, we have learned that the prediction of the temperature-induced incommensurate-to-commensurate phase transition in the Cr spacer has been confirmed by neutron scattering measurements reported by J.F. Ankner *et al.* at the 41st Annual Conference on Magnetism & Magnetic Materials.

- [1] E. Fawcett, *Rev. Mod. Phys.* **60**, 209 (1988); E. Fawcett *et al.*, *Rev. Mod. Phys.* **66**, 25 (1994).
- [2] J. Ungris, R.J. Celotta, and D.T. Pierce, *Phys. Rev. Lett.* **69**, 1125 (1992); **67**, 140 (1991).
- [3] J. Meersschaut *et al.*, *Phys. Rev. Lett.* **75**, 1638 (1995).
- [4] M. van Schilfgaarde and F. Herman, *Phys. Rev. Lett.* **71**, 1923 (1993); D. Stoeffler and F. Gautier, *Phys. Rev. B* **44**, 10389 (1991).
- [5] P.A. Fedders and P.C. Martin, *Phys. Rev.* **143**, 245 (1966).
- [6] R.S. Fishman and S.H. Liu, *Phys. Rev. B* **48**, 3820 (1993).
- [7] D.G. Laurent, J. Callaway, J.L. Fry, and N.E. Brener, *Phys. Rev. B* **23**, 4977 (1981).
- [8] Assuming a helicoidal antiferromagnetic SDW in the Cr spacer, Slonczewski proposed a noncollinear in-plane coupling between two proximity magnetic layers [J.C. Slonczewski, *J. Magn. Magn. Mater.* **150**, 13 (1995)].
- [9] The density of states on the nested electron and hole Fermi surfaces in the thin spacer is probably close to that in the bulk. Then ρ_{eh} is in the range of 2.4–3.7 states/atom Ry for bulk Cr [N.I. Kulikov and E.T. Kulatov, *J. Phys. F* **12**, 2291 (1982)]. If $\rho_{eh} = 3.7$ states/atom Ry and $S_M = 2.2$ (for Fe), then $\gamma \approx 2.5$ when A is 30 meV. By comparison, the coupling between two neighboring (001) Fe planes is $A \approx -100$ meV.
- [10] See, for example, A. Fetter and J. Walecka, *Quantum Theory of Many-Particle Systems* (McGraw Hill, New York, 1971), p. 426.
- [11] S. Mirbt, A.M.N. Niklasson, B. Johansson, and H.L. Skriver, *Phys. Rev. B* **54**, 6382 (1996).
- [12] Z. Zhang, L. Zhou, P.E. Wigen, and K. Ounadjela, *Phys. Rev. Lett.* **73**, 336 (1994).
- [13] E.E. Fullerton, J.E. Mattson, C.H. Sowers, and S.D. Bader, *Scr. Metall. Mater.* **33**, 1637 (1995).
- [14] Y. Henry and K. Ounadjela, *Phys. Rev. Lett.* **76**, 1944 (1996).
- [15] E.E. Fullerton, S.D. Bader, and J.L. Robertson, *Phys. Rev. Lett.* **77**, 1382 (1996).
- [16] T.G. Walker, A.W. Pang, H. Hopster, and S.F. Alvarado, *Phys. Rev. Lett.* **69**, 1121 (1992); C. Turtur and G. Bayreuther, *Phys. Rev. Lett.* **72**, 1557 (1994).
- [17] R.S. Fishman and S.H. Liu, *Phys. Rev. B* **50**, 4240 (1994); *Phys. Rev. Lett.* **76**, 2398 (1996).